ISSN 0036-0236, Russian Journal of Inorganic Chemistry, 2012, Vol. 57, No. 8, pp. 1079–1088. © Pleiades Publishing, Ltd., 2012.

COORDINATION COMPOUNDS

Peroxo Complexes of Uranium(VI) Containing Nitrogen and Oxygen Donor Ligands[1]

Balgar Singh, Simpy Mahajan, H. N. Sheikh, Mohita Sharma, and Bansi Lal Kalsotra

Department of Chemistry, University of Jammu, Jammu-1800 06 (India)

e-mail: hnsheikh@rediffmail com

Received December 28, 2010

Abstract—The uranium(VI) peroxo complexes containing Mannich base ligands having composition $[UO(O_2)L\text{-}L(NO_3)_2]$ {where L-L = morpholinobenzyl acetamide (MBA), piperidinobenzyl acetamide (PBA), morpholinobenzyl benzamide (MBB), piperidinobenzyl benzamide (PBB), morpholinomethyl benzamide (MMB), piperidinomethyl benzamide (PMB), morpholinobenzyl formamide (MBF), piperidinobenzyl formamide (PBF)} are reported. In a typical reaction $UO_2(NO_3)_2 \cdot 6H_2O$ (1 mmol, 0.502 g) was dissolved in methanol. An equimolar (1 mmol) methanolic solution (30 mL) of the ligand (Mannich bases) was added to a solution of uranyl nitrate followed by addition of potassium hydroxide (KOH) (2 mmol, 0.1122 g). The solution was refluxed for 15 min and then 10 mL of 30% hydrogen peroxide (H_2O_2) was added dropwise and was refluxed for an additional 1 h. The synthesized complexes have been characterized by various physico-chemical techniques, viz. elemental analysis, molar conductivity, magnetic susceptibility measurements, infra red, electronic, mass spectral and TGA/DTA studies. These studies revealed that the synthesized complexes are non-electrolytic and diamagnetic in nature. The ligands are bound to metal in a bidentate mode through carbonyl oxygen and the ring nitrogen. Thermal analysis result provides conclusive evidence for the absence of water molecule in the complexes. Mass spectra confirm the molecular mass of the complexes. Antibacterial activity of complexes revealed enhanced activity of complexes as compared to corresponding free ligands. Molecular modeling suggests pentagonal bipyramidal structure for complexes.

DOI: 10.1134/S003602361208013X

Metal peroxo complexes have been the object of intense investigation for the past several years, for a variety of reasons including their role as oxidation catalyst [1, 2] and biochemical relevance [3–10]. They are widely used in stoichiometric as well as catalytic oxidation in organic and biochemistry [11], for example in the oxidation of thioanisole [12, 13], methylbenzenes [14], tertiary amines, alkenes, alcohols [15, 16], bromide [17] and also in olefin epoxidations [18–22]. Peroxo complexes of molybdenum and tungsten are attracting interest as oxidants in organic synthesis [23]. As uranium somewhat resembles the group VIB elements, it was of interest to discover whether it would form analogous peroxo complexes which contain organic moieties. The preeminence of the UO_2 group distinguishes uranium from molybdenum and tungsten, however, and this factor may have hitherto prevented the generation of peroxo complexes from uranyl salts and organic reagents. Various peroxo complexes of uranium have been reported with organic ligands [24]. The coordination number for metal chelates of Th(IV) and UO_2(VI) have been reported [25, 26].

Metal complexes of Mannich bases have played a vital role in the development of coordination chemistry [27, 28]. Studies on metal complexes of the formaldehyde and benzaldehyde-based Mannich bases have already been reported [29]. The synthesis of N-(morpholinobenzyl) benzamide and its complexation with CuII, CoII, NiII and ZnII has been reported [30]. In the present manuscript we describe the synthesis and characterization of peroxo complexes of uranium(VI) with some formaldehyde and benzaldehyde-based Mannich base ligands. The structures of ligands are given in scheme.

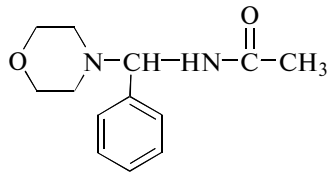

MBA

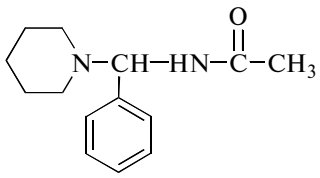

PBA

Scheme 1. Structure of ligands.

[1] The article is published in the original.

EXPERIMENTAL

All the reagents used were chemically pure and of analytical reagent grade. Solvents used were purified and dried according to standard procedures [31]. Dimethyl sulphoxide (Ranbaxy), dimethyl formamide (Qualigens), and ethanol (commercial) were used after distillation; morpholine (Ranbaxy), piperidine (SDS), benzaldehyde (Ranbaxy), benzamide (Thomas Baker), acetamide (Ranbaxy), formaldehyde (Ranbaxy), formamide (Loba), uranyl nitrate (SISCO) and hydrogen peroxide (Merck) were used as supplied. The ligands were prepared by the reported method [30, 32]. The analysis of uranium was carried out gravimetrically as uranyl oxinate $UO_2(C_9H_6ON)_2C_9H_7ON$ after decomposing the complex with concentrated nitric acid [31]. Carbon, hydrogen, nitrogen were analyzed micro analytically using CHNS analyzer Leco Model-932. The total peroxide content of the complexes was determined by adding a weighed amount of the compound to a cold solution of 1.5% boric acid (w/v) in 0.7 M sulfuric acid (100 mL) and then titrating against standard Cerium(IV) solution [33]. Molar conductivity of complexes was measured at room temperature by a Digital Conductivity Meter of model 611E having a conductivity cell with a cell constant of 1.0 + 10% using 10^{-3} molar solution of complexes in DMF. Magnetic susceptibility measurements were carried out by Gouy's method at room temperature using $Hg[Co(NCS)_4]$ as standard. IR spectra of complexes over the region 400–4000 cm^{-1} were recorded on Perkin Elmer's FTIR spectrophotometer model RX1, using KBr discs. Melting points were determined on Analab melting point apparatus and are corrected should be replaced by corrected. Mass spectral data were obtained on ESI-esquires 3000 Bruker Daltonics spectrometer. Electronic spectra over the region 200–900 nm were recorded by UV-visible single beam spectrophotometer systronics using 10^{-3} M DMF solution of complexes. TGA/DTA studies were recorded on Linseis STA PT-1000 (Pyris Diamond) thermoanalyser at the heating rate of 10°C per minute in an atmosphere of air in the temperature range 23–1000°C.

Preparation of ligands. The ligands MBA, PBA, MBB, PBB, MMB, PMB, MBF, PBF were prepared by the reported method [30]. In a typical reaction acetamide/benzamide/formamide (0.1 mol) in 20 mL of ethanol was mixed with piperidine/morpholine (0.1 mol) with constant stirring to get a clear solution under ice cooled condition. To the resulting solution, benzaldehyde/formaldehyde (0.1 mol) was added dropwise with stirring for 15–20 min under ice cooled condition.

The reaction mixture was then kept at room temperature for 2 days. The colourless solid obtained was filtered, washed with distilled water and recrystallized from ethanol.

Preparation of uranyl peroxo complexes. The peroxo complexes were synthesized by reported procedure [34]. In a typical reaction $UO_2(NO_3)_2 \cdot 6H_2O$ (1 mmol, 0.502 g) was dissolved in methanol. An equimolar (1 mmol) methanolic solution (30 mL) of the ligand (Mannich bases) {MBA (0.234 g), PBA (0.232 g), MBB (0.296 g), PBB (0.294 g), MBF (0.220 g), PBF (0.218 g), MMB (0.220 g), PMB (0.218 g)} was added to a solution of uranyl nitrate solution followed by addition of potassium hydroxide (KOH) (2 mmol, 0.1122 g). The solution was refluxed for 15 min. Then 10 mL of 30% H_2O_2 was added dropwise and was refluxed for an additional 1 h. The resulting yellow coloured precipitates were filtered after cooling and washed successively with methanol, ether and dried in vacuo.

$$UO_2(NO_3)_2 \cdot 6H_2O + H_2O_2 + \text{L-L} \rightarrow [UO(O_2)\text{L-L}(NO_3)_2] + 7H_2O$$

Antimicrobial study. The invitro biological screening effects of the investigated compounds (Table 6) were tested against two bacteria viz. *Staphylococcus aureus* and *Escherichia coli*. The paper disc plate method (disc diffusion method) described by Skinner was employed to evaluate bactericidal activity using agar nutrient as the medium. The test solutions were prepared by dissolving the ligands in ethanol and the complexes in DMF. In a typical procedure, discs of filter paper were dipped into the solution of each chemical separately for two hours. Seeded petri plates were then prepared by pouring the nutrient agar medium in each petri plate, followed by inoculation of bacterial suspension. After the solidification of the medium, the discs of chemicals were put on seeded plates and the plates were incubated at 25°C for 24 h. PDA mixed with test solution was poured into sterilized petriplates.

RESULTS AND DISCUSSION

The analytical and spectroscopic results (Tables 1–3) showed that all complexes have general formula $[UO(O_2)\text{L-L}(NO_3)_2]$ (where L-L = MBA, PBA, MBB, PBB, MMB, PMB, MBF, PBF). The isolated solid complexes are stable to air and light and are insoluble in common organic solvents but soluble in DMSO and DMF. All the complexes are yellowish colored. All complexes decompose on heating and do not have sharp melting points.

Conductance and magnetic measurements. The molar conductivity values, λ_M of the complexes (Table 1) measured in DMF solution lie in the range of 8–13 $ohm^{-1}\ cm^2\ mol^{-1}$ which indicates the non-electrolytic nature of these complexes [35]. Moreover, magnetic studies show that all the complexes are diamagnetic as expected for d^0 system of uranyl(VI) peroxo complexes.

IR spectra. The characteristic IR absorptions and their assignments for the ligand and metal are given in Table 2. The IR spectra of all the complexes exhibit

Table 1. Analytical data and some physical properties of uranium(VI) peroxo complexes

Complex	Empirical formula (formula wt.) g mol^{-1}	Colour	Dec. temp. (°C)	Found			(Calcd.) %		λ_M (Ohm^{-1} cm^2 mol^{-1})
				C	H	N	O_2^{2-}	U	
$[UO(O_2)MBA(NO_3)_2]$	$UC_{13}H_{18}N_4O_{11}$	Yellow	>320	24.19	2.73	8.66	4.95	36.90	8
	(644)			(24.23)	(2.80)	(8.70)	(4.97)	(36.96)	
$[UO(O_2)PBA(NO_3)_2]$	$UC_{14}H_{20}N_4O_{10}$	Greenish yellow	>335	26.11	3.08	8.70	4.95	37.00	10
	(642)			(26.16)	(3.12)	(8.72)	(4.98)	(37.07)	
$[UO(O_2)MBB(NO_3)_2]$	$UC_{18}H_{20}N_4O_{10}$	Yellow	>345	30.52	2.80	7.89	4.50	33.68	13
	(704)			(30.59)	(2.83)	(7.93)	(4.53)	(33.71)	
$[UO(O_2)PBB(NO_3)_2]$	$UC_{19}H_{22}N_4O_{10}$	Yellow	>331	32.36	3.10	7.91	4.50	33.78	11
	(704)			(32.39)	(3.13)	(7.95)	(4.55)	(33.81)	
$[UO(O_2)MMB(NO_3)_2$	$UC_{12}H_{16}N_4O_{11}$	Yellow	>340	22.82	2.50	8.85	5.05	37.75	8
	(630)			(22.86)	(2.54)	(8.89)	(5.08)	(37.78)	
$[UO(O_2)PMB(NO_3)_2$	$UC_{13}H_{18}N_4O_{10}$	Yellow	>337	24.80	2.82	8.90	5.06	37.86	9
	(628)			(24.84)	(2.87)	(8.92)	(5.10)	(37.90)	
$[UO(O_2)MBF(NO_3)_2]$	$UC_{12}H_{16}N_4O_9$	Yellow	>343	28.21	2.65	9.33	5.33	39.75	12
	(598)			(28.23)	(2.68)	(9.36)	(5.35)	(39.80)	
$[UO(O_2)PBF(NO_3)_2$	$UC_7H_{14}N_4O_{10}$	Yellow	>345	15.19	2.51	10.11	5.26	43.09	10
	(552)			(15.22)	(2.54)	(10.14)	(5.30)	(43.12)	

bands characteristic of the coordinated oxo, peroxo groups and the ligand molecule. The metal peroxo group gives rise to three IR active vibrational modes. These are due to ν(O–O), $\nu_{asym}(UO_2)$ and $\nu_{sym}(UO_2)$. These characteristic vibration modes appear around 861–900, 669–707 and 460–508 cm^{-1} respectively in complexes. These bands confirm the η^2-coordination of the peroxo group [36]. In all complexes, an additional sharp band around 930–973 cm^{-1} has been assigned to ν(U=O) mode [3] and [24]. Thus, IR spectra confirms the presence of $[UO(O_2)]^{2+}$ moiety in these complexes.

In order to study the binding mode of Mannich base ligands with uranium in the peroxo complexes, the IR spectra of the free ligands were compared with those of corresponding metal complexes (Table 2).

In MBA and PBA ligands, a sharp band at 1641 and 1631 cm^{-1} appeared due to ν(C=O) of amide group respectively and another band assigned to ν(C–N–C) of morpholine and piperidine rings appeared at 1111 and 1138 cm^{-1} respectively (Table 2). Also, bands at 3121 and 3161 cm^{-1} appeared due to ν(N-H) stretching of ligands. In the corresponding complexes $[UO(O_2)MBA(NO_3)_2]$ and $[UO(O_2)PBA(NO_3)_2]$, these bands appear at lower frequencies at 1631, 1621, 1104, 1112, 3080 and 3156 cm^{-1} respectively indicating bonding of the ligands through carbonyl oxygen and ring nitrogen of morpholine/piperidine (Table 2). Ring nitrogens of alicyclic amines in various ligands have been reported to coordinate metal ion [37].

In MBB and PBB ligands, a sharp band due to ν(C=O) of amide group appeared at 1631 and 1637 cm^{-1} respectively and band due to ν(C–N–C) of morpholine and piperidine rings appeared at 1137 and 1120 cm^{-1} respectively. Another band due to ν(N–H) stretching appeared at 3174 and 3180 cm^{-1} respectively. In both the complexes $[UO(O_2)MBB(NO_3)_2]$ and $[UO(O_2)PBB(NO_3)_2]$, the ν(C=O) band appeared at 1630 and 1625 cm^{-1}, the band due to ν(C–N–C) of morpholine and piperidine rings appeared at 1129 and 1113 cm^{-1} respectively. The band due to ν(N–H) stretching appeared at 3155 and 3167 cm^{-1} respectively. All the bands exhibit negative shifts relative to their corresponding positions in free ligands, indicating the coordination through carbonyl oxygen and ring nitrogen [38].

In MMB and PMB ligands, ν(C=O) appeared at 1639 and 1640 cm^{-1}, ν(C–N–C) of morpholine and piperidine rings appeared at 1150 and 1113 cm^{-1} and another band due to ν(N–H) stretching appeared at 3058 and 3056 cm^{-1} respectively. In both the complexes $[UO(O_2)MMB(NO_3)_2]$ and $[UO(O_2)PBB(NO_3)_2]$,

Table 2. IR Spectral data (cm^{-1}) of uranium(VI) peroxo complexes

Ligand	ν(NH)	ν(C–N–C)	ν(C=O)	Complex	ν(NH)	ν(C–N–C)	ν(O–O)	ν(U=O)	ν(O–O)	$\nu_{asym}(UO_2)$	$\nu_{sym}(UO_2)$
MBA	3121	1111	1641	$[UO(O_2)MBA(NO_3)_2]$	3080	1104	1631	970	892	707	460
PBA	3161	1138	1631	$[UO(O_2)PBA(NO_3)_2]$	3156	1112	1621	969	900	696	480
MBB	3174	1137	1631	$[UO(O_2)MBB(NO_3)_2]$	3155	1129	1630	973	898	690	508
PBB	3180	1120	1637	$[UO(O_2)PBB(NO_3)_2]$	3167	1113	1625	965	891	669	477
MMB	3058	1150	1639	$[UO(O_2)MMB(NO_3)_2]$	3045	1145	1631	930	861	700	500
PMB	3056	1113	1640	$[UO(O_2)PMB(NO_3)_2]$	3039	1129	1633	961	879	672	502
MBF	2971	1138	1631	$[UO(O_2)MBF(NO_3)_2]$	2961	1132	1626	955	870	697	490
PBF	3027	1116	1644	$[UO(O_2)PBF(NO_3)_2]$	3015	1108	1632	975	885	665	497

Table 3. Mass spectral data of uranium(VI) peroxo complexes

Complex (**1**) $[UO(O_2)C_{13}H_{18}N_4O_8]$ (644.34 g mol^{-1})	m/e (%)	M-3* (%)	M* (%)	M+1* (%)	M+2* (%)	Complex (**2**) $[UO(O_2)C_{18}H_{20}N_4O_8$ (706.41 $gmol^{-1}$)	m/e (%)	M-3* (%)	M* (%)	M+1* (%)	M+2* (%)
$[UO(O_2)C_{13}H_{18}N_4O_8]^+$	643.34 (16.36)	0.70	100	16.2	3.5	$[UO(O_2)C_{18}H_{20}N_4O_8]^+$	705.41 (1.60)	0.70	100	21.6	4.5
$[UOC_{13}H_{18}N_4O_8]^+$	611.34 (15.45)	0.70	100	16.1	3.0	$[UOC_{18}H_{20}N_4O_8]^+$	673.41 (0.83)	0.70	100	21.5	4.0
$[UOC_{13}H_{18}N_3O_5]^+$	549.33 (9.09)	0.70	100	15.6	2.4	$[UOC_{18}H_{20}N_3O_5]^+$	611.40 (7.50)	0.70	100	21.0	3.3
$[UOC_{13}H_{18}N_2O_2]^+$	487.32 (19.99)	0.70	100	15.1	1.7	$[UOC_{18}H_{20}N_2O_2]^+$	549.39 (33.33)	0.70	100	20.5	2.6
$[UC_{13}H_{18}N_2O_2]^+$	471.32 (15.40)	0.70	100	15.0	1.5	$[UC_{18}H_{20}N_2O_2]^+$	533.39 (14.16)	0.70	100	20.5	2.4
$[UC_7H_{13}N_2O_2]^+$	394.32 (20.90)	0.70	100	8.5	0.7	$[UC_{12}H_{15}N_2O_2]^+$	456.39 (14.99)	0.70	100	13.9	1.3
$[UC_6H_{11}NO_2]^+$	366.31 (36.36)	0.70	100	7.1	0.6	$[UC_{11}H_{13}NO_2]^+$	428.38 (9.16)	0.70	100	12.5	1.1
$[UC_5H_8NO]^+$	322.33 (100)	0.70	100	5.9	0.3	$[UC_5H_8NO]^+$	323.38 (100)	0.70	100	4.8	0.3

* Relative asotopic abundances.

Table 4. Electronic Spectral data (nm) of uranium(VI) peroxo complexes

S. No.	Complex	λ (nm)
1.	$[UO(O_2)MBA(NO_3)_2]$	307, 331, 357
2.	$[UO(O_2)PBA(NO_3)_2]$	314, 329, 354
3.	$[UO(O_2)MBB(NO_3)_2]$	308, 332, 357
4.	$[UO(O_2)PBB(NO_3)_2]$	310, 330, 355
5.	$[UO(O_2)MMB(NO_3)_2]$	313, 320, 353
6.	$[UO(O_2)PMB(NO_3)_2]$	311, 335, 360
7.	$[UO(O_2)MBF(NO_3)_2]$	306, 337, 361
8.	$[UO(O_2)PBF(NO_3)_2]$	305, 340, 359

these bands appeared at lower frequencies, i.e., ν(C=O) band at 1631 and 1633 cm^{-1}, ν(C–N–C) at 1145 and 1109 cm^{-1} and ν(N–H) stretching band at 3045 and 3039 cm^{-1} respectively, indicating the coordination through carbonyl oxygen and ring nitrogen.

In MBF and PBF ligands, a sharp band due to ν(C=O) of amide group appeared at 1631 and 1644 cm^{-1}, band due to ν(C–N–C) of morpholine and piperidine rings appeared at 1138 and 1116 cm^{-1} and another band due to ν(N–H) stretching appeared at 2971 and 3027 cm^{-1} respectively. In both the complexes $[UO(O_2)MBF(NO_3)_2]$ and $[UO(O_2)PBF(NO_3)_2]$, these bands appeared at lower frequencies, i.e., ν(C=O) band at 1626 and 1632 cm^{-1}, the ν(C–N–C) band at 1129 and 1108 cm^{-1} and the ν(N–H) stretching band at 2961 and 3015 cm^{-1} respectively, indicating the coordination through carbonyl oxygen and ring nitrogen. Thus, IR spectra confirm that the ligands are coordinated to uranium in a bidentate chelating mode.

In these complexes three additional bands which are not present in the spectra of free ligands are observed. Of these a band appears around 985–980 cm^{-1} assigned to $\nu_s(NO)$ (ν_2) mode of NO_3^- group. Two more bands in the region 1466–1458 and 1376–1384 cm^{-1} of the coordinated nitrato group are assigned as $\nu_a(NO_2)$ ν_5 and $\nu_s(NO_2)$ ν_1 modes respectively. A difference in frequencies between the higher energy bands ($\Delta\nu$ ($\nu_5 - \nu_1$) ≈ 82 cm^{-1}), suggests unidentate coordination of the nitrato group [39, 40]. For bidentate coordination of nitrato group, the difference should be of the order 180 cm^{-1} [38].

TGA/DTA. TGA and DTA thermogram are recorded up to 1000°C for a representative complex $[UO(O_2)MBA(NO_3)_2]$ at a heating rate of 10°C/min. The TG curve (Fig. 1) for the complex corresponds to weight loss of 14.0%. This weight loss approximates to loss of peroxo and nitrate group (theoretical weight loss 14.6%). Further heating up to 1000°C shows a gradual weight loss of 2.3% (theoretical weight loss 2.5%) attributable to loss of oxo group. A broad exothermic curve all along indicates oxidation of ligand and decomposition of complex.

ESI mass spectra. The ESI mass spectra have been recorded for complexes $[UO(O_2)MBA(NO_3)_2]$ (**1**) and $[UO(O_2)MBB(NO_3)_2]$ (**2**). Both the complexes show extensive fragmentation and only the most abundant fragment ions with relative isotopic abundance are given in Table 3. The complex (**1**) displayed molecular ion peak at m/e 643.34 for fragment $[UO(O_2)C_{13}H_{18}N_4O_8]^+$ and the complex (**2**) at m/e 705.41 for fragment $[UO(O_2)C_{18}H_{20}N_4O_8]^+$.

Masses of fragment ions listed in table are calculated using uranium atom mass equal to 238.05 amu. For complex (**1**) base peak appears at m/e 322.33 corresponding to $[UC_5H_8NO]^+$ and for complex (**2**) it

Table 5. Selected bond lengths and bond angles for the complex $[UO(O_2)MBA(NO_3)_2]$

Bond	Bond length (Å)	Angle	Bond angles (°)
N(5)–U(35)	2.14505	N(5)U(35)O(16)	83.55
O(16)–U(35)	2.04156	N(5)U(35)O(36)	120.55
O(36)–U(35)	1.98006	O(36)U(35)O(16)	52.599
O(37)–U(35)	2.08295	O(36)U(35)O(40)	63.082
O(38)–U(35)	2.08536	O(36)U(35)O(39)	110.13
O(39)–U(35)	2.08533	O(36)U(35)O(38)	70.884
O(40)–U(35)	2.09828	O(36)U(35)O(37)	54.857
O(37)–O(38)	1.30327	O(16)U(35)O(37)	92.713
O(39)–N(41)	1.33671	O(38)U(35)O(37)	36.439
O(40)–N(42)	1.34338	O(16)U(35)O(40)	58.827

appears at m/e 323.38 corresponding to $[UC_5H_8NO]^+$.

Uranium has two isotopes having atomic masses 235 and 238 amu. Their relative abundances are 0.70 and 100% respectively. Here, the most intense isotope peak is set to 100% and percentages of other isotope peaks are computed relative to it (Table 3). The molecular ion and fragments peaks containing uranium appear in doublet at M+* and M-3* and ratios of their relative intensities confirm the presence of U-235 and U-238 isotopes in the fragments. In addition M+1* and M+2* peaks also appear due to isotopic contribution of C, H, N and O atoms.

Electronic spectra. The electronic spectra of the metal complexes were recorded in 10^{-3} M DMF solution (Table 4) in the UV-visible region. The spectra show three transitions in the range 305–314, 320–340 and 353–361 nm ascribed to $\pi \rightarrow \pi^*$, $n \rightarrow \pi^*$ and the charge transfer transitions from uranyl oxygen $\rightarrow$ uranium, i.e. LMCT, $\pi\, O_2^{2-} \rightarrow U$ [35] and [41]. There was no evidence of any d–d transition. This result is consistent with the presence of uranium(VI) system in the complexes.

Molecular modeling. Since single crystals could not be grown for these complexes, it was thought worthwhile to obtain structural information through molecular modeling. The molecular modeling calculations for the complex, $[UO(O_2)MBA(NO_3)_2]$, has been carried out using Hyperchem release 8.0 professional version, which allows for rapid structural building, geometry optimization, and molecular display [42]. Energy values obtained for the complex indicate pentagonal bipyramidal geometry. Figures 2a and 2b show the energy-minimized structure for complex, $[UO(O_2)MBA(NO_3)_2]$. The lowest energy values obtained from this study for the complex, $[UO(O_2)MBA(NO_3)_2]$ is 317.599 kcal mol^{-1}. Selected bond lengths (Å) and bond angles (°) obtained from the energy-minimized structures are given in Table 5. The probable structure thus exhibit molecular properties in conformity with experimentally determined data.

Table 6. Antibacterial activity of the ligands and their complexes at 200 ppm

S. No.	Compound	Zone of inhibition in mm	
		Staphylococcus aureus	*Escherichia coli*
1.	PBA(L1)	1.4	0.8
2.	PBB(L2)	1.8	0.6
3.	$[UO(O_2)PBA(NO_3)2]$ (UL1)	2.3	1.8
4.	$[UO(O_2)PBB(NO_3)_2]$ (UL2)	2.9	1.3
5.	Control	4.5	1.2

On the basis of analytical, IR, UV-Vis. and mass spectral data combined with molecular modeling calculations, a pentagonal bipyramidal geometry has been proposed and the representative structure for the complex, $[UO(O_2)MBA(NO_3)_2]$, is given in Figs. 2a, 2b.

Antibacterial study. The in vitro biological screening effects of the ligands and the corresponding complexes were tested against two bacteria viz. *Staphylococcus aureus* and *Escherichia coli*. The paper disc plate method (disc diffusion method) [43] described by Skinner was employed to evaluate bactericidal activity using agar nutrient as the medium. The test solutions were prepared by dissolving the ligands in ethanol and the complexes in DMF. In a typical procedure, discs of filter paper were dipped into the solution of each chemical separately for 2 h. Seeded petri plates were then prepared by pouring the nutrient agar

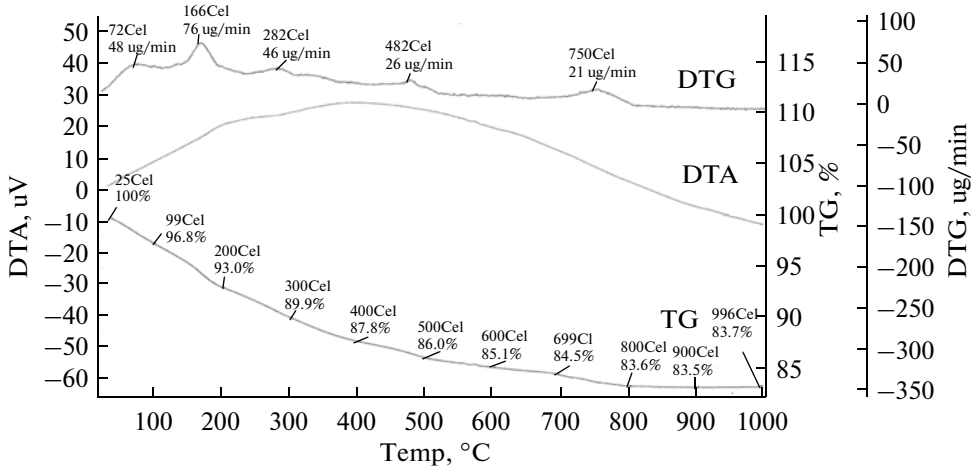

Fig. 1. TGA/DTA thermogram of $[UO(O_2)MBA(NO_3)_2]$.

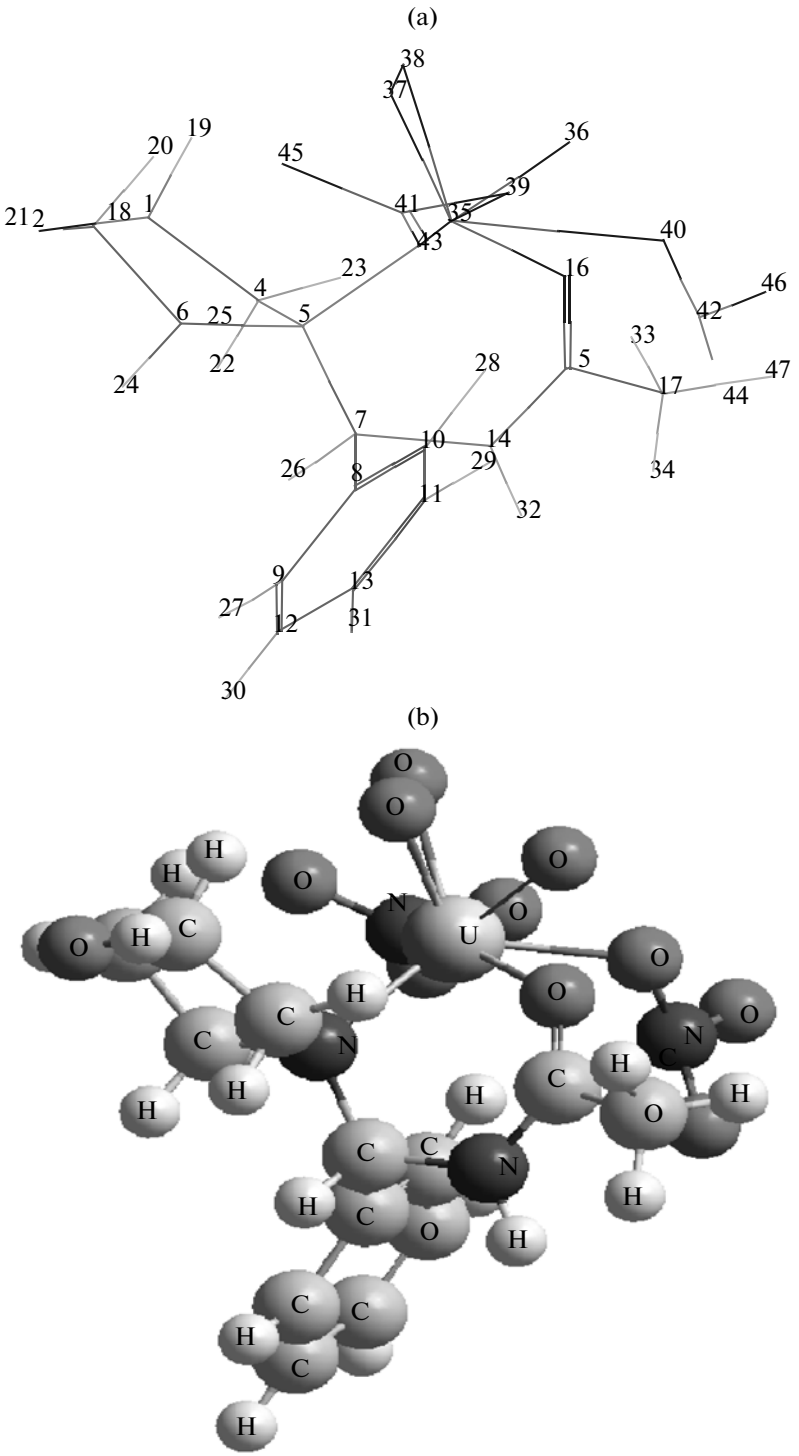

Fig. 2. (a) Atomic labeling; (b) Energy minimized structure of the complex, $[UO(O_2)MBA(NO_3)_2]$.

medium in each petri plate, followed by inoculation of bacterial suspension. After the solidification of the medium, the discs of chemicals were put on seeded plates and the plates were incubated at 25°C for 24 h. During this period, the test solution was diffused and the growth of the inoculated microorganisms was affected. The inhibition zone (clear area around the disc) developed on each plate was measured (Fig. 3). The work was carried out under aseptic conditions and a standard antibiotic Rifampicin was used as the con-

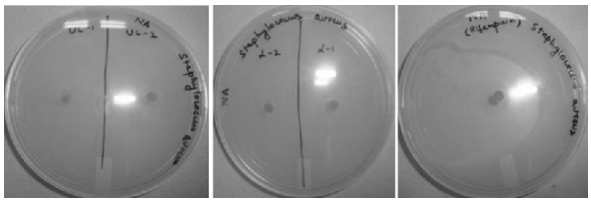

(L1/L2) Control (Rifampicin) (UL1/UL2)

Antibacterial studies of ligands and complexes against *Staphylococcus aureus*

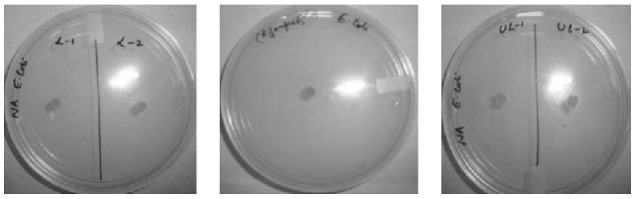

(L1/L2) Control (Rifampicin) (UL1/UL2)

Antibacterial studies of ligands and complexes against *Escherichia coli*

Fig. 3. Antibacterial activity of the ligands and their complexes at 200 ppm.

trol. A comparative study of the ligands with the complexes indicates that the complexes exhibit higher activity than the free ligands (Table 6).

Therefore, the metal complexes are more potent than the parent ligands. The chelation theory accounts for the increased activity of the metal complexes [44]. Chelation reduces the polarity of the metal atom mainly because of partial sharing of its positive charge with the donor groups, thereby, increasing the liphophilic nature of the central atom which subsequently favours its permeation through the lipid layer of the cell membrane. Blank tests showed that ethanol and DMF used in the preparation of the test solutions does not affect the test organism. Each treatment was repeated three times to minimize error and average data were taken as the final result.

REFERENCES

1. A. Butler, M. J. Clague, and G.E. Meister, Chem. Rev. **94**, 625 (1994).
2. H. Mimoun, M. Mignard, P. Brechot, and L. Saussine, J. Am. Chem. Soc. **108**, 3711 (1986).
3. D. C. Crans, J. J. Smee, E. Gaidamauskas, and L. Yang, Chem. Rev. **104**, 849 (2004).
4. K. H. Thompson, J. H. McNeill, and C. Orvig, Chem. Rev. **99**, 2561 (1999).
5. K. H. Thompson and C. Orvig, J. Chem. Soc., Dalton Trans., 2885 (2000).
6. A. K. Haldar, S. Banerjee, K. Naskar, et al., Exp. Parasitology **122**, 145 (2009).
7. M. Saleem, M. Sharma, H. N. Sheikh, and B. L. Kalsotra, Ind. J. Chem. A **46**, 1423 (2007).
8. M. Sharma, H. N. Sheikh, M. S. Pathania, and B. L. Kalsotra, J. Coord. Chem. **61**, 426 (2008).
9. D. Kalita, S. Sarmah, S. P. Das, et al., React. Funct. Polym. **68**, 876 (2008).
10. M. Sharma, M. Saleem, M. S. Pathania, et al., Chin. J. Chem. **27**, 311 (2009).
11. B. Tamani and H. Yeganeh, Eur. Polym. J. **35**, 1445 (1999).
12. M. Chiarini, N. D. Gillitt, and C. A. Bunton, Langmuir **18**, 3836 (2002).
13. C. A. Bunton and N. D. Gillitt, J. Phys. Org. Chem. **15**, 29 (2002).
14. R. Bandyopadhyay, S. Biswas, S. Guha, et al., Chem. Commun., 1627 (1999).
15. O. S. Bortolini, S. F. D. Compestrini, F. D. Furia, and G. Modena, J. Org. Chem. **52**, 5467 (1987).
16. A. J. Bailey, W. P. Griffith, B. C. Parkin, J. Chem. Soc. Dalton Trans., 1833 (1995).
17. M. S. Reynolds, S. J. Morandi, J. W. Raebiger, et al., Inorg. Chem. **33**, 4977 (1994).
18. D. V. Deubel, J. Sundermeyer, and G. Frenking, J. Org. Chem. **65**, 2996 (2000).
19. G. Wahl, D. Kleinhenz, A. Schorm, et al., Chem. Eur. J. **5**, 3237 (1999).
20. J. Cross, P. D. Newman, R. D. Peacock, and D. Stirling, J. Mol. Catal. A: Chem. **144**, 273 (1999).
21. D. V. Deubel, J. Sundermeyer, and G. Frenking, J. Am. Chem. Soc. **122**, 10101 (2000).
22. X. Y. Wang, H. C. Shi, and S. Y. Xu, J. Mol. Catal. A: Chem. **206**, 213 (2003).
23. A. D. Westland and M. T. H. Tarafder, Inorg. Chem. **20**, 3992 (1981).
24. S. M. Islam, M. Begum, H. N. Roy, et al., Synth. React. Inorg. Met.-Org. Chem. **27**, 17 (1997).

25. S. A. Abdel Latif, Synth. React. Inorg. Met.-Org. Nano-Met. Chem. **31**, 1355 (2001).

26. A. D. Keramidas, M. P. Rikkou, C. Drouza, et al., J. Radiochem. Acta **90**, 549 (2002).

27. N. Raman and S. Ravichandran, Polish J. Chem. **78**, 2005 (2004).

28. N. Raman and S. Ravichandran, Asian J. Chem. **15**, 1848 (2003).

29. A. Ravichandran and D. Venkappayya, J. Ind. Chem. Soc. **67**, 584 (1990).

30. N. Raman, R. Vimalaramani, and C. Thangaraja, Ind. J. Chem. **43**, 2357 (2004).

31. A. I. Vogel, *Quantitative Inorganic Analysis* (ELBS and Longman, London, 1978).

32. G. Venkatesa Prabhu and D. Venkappayya, J. Ind. Chem. Soc. **72**, 511 (1985).

33. M. K. Chaudhuri, S. K. Ghosh, and N. S. Islam, Inorg. Chem. **24**, 2706 (1985).

34. M. T. H. Tarafder and A. M. Anwarul Islam, Polyhedron **8**, 109 (1989).

35. D. A. Chowdhury, M. N. Uddin, M. A. H. Sarker, Chiang Mai J. Sci. **35**, 483 (2008).

36. C. Djordjevic, N. Vuletic, B. A. Jacobs, and E. Sin, Inorg. Chem. **36**, 1798 (1997).

37. H. N. Sheikh, A. Hussain, and B. L. Kalsotra, Russ. J. Inorg. Chem. **51**, 724 (2006).

38. K. Nakamoto, *IR and Raman Spectra of Inorganic and Coordination Compounds*, 4th ed. (Wiley, New York, 1986).

39. B. N. Gatehouse, S. E. Livingstone, and R. S. Nyholm, J. Chem. Soc. **5**, 4222 (1957).

40. N. F. Curtis and Y. M. Curtis, Inorg. Chem. **4**, 804 (1965).

41. G. A. Thakur, S. V. Athlekar, S. R. Dharwadker, and M. M. Shaikh, Acta Polon. Pharm.-Drug Res. **64**, 9 (2007).

42. G. R. Brubaker and D. W. Johnson, Coord. Chem. Rev. **53**, 1 (1984).

43. M. S. Rahman and M. N. Anwar, Bangladesh J. Microbiol. **24**, 73 (2007).

44. R. Gupta, H. N. Sheikh, M. Sharma, and B. L. Kalsotra, J. Coord. Chem. **63**, 3256 (2010).